

## Radiation Induced Degradation of SOI n-channel LDMOSFETs

J.F. Conley, Jr.,<sup>1</sup> A. Vandooren,<sup>2</sup> L. Reiner,<sup>3</sup> S. Cristoloveanu,<sup>4</sup> M. Mojarradi,<sup>1</sup> and E. Kolowa<sup>1</sup>

<sup>1</sup>California Institute of Technology, Jet Propulsion Lab, Pasadena, CA 91109

<sup>2</sup>Digital DNA Labs, Motorola Inc., Austin TX 78721.

<sup>3</sup>California State University Northridge, Northridge, CA 91325

<sup>4</sup>LPCS / ENSERG, 38016 Grenoble Cedex, France

SOI Laterally Diffused MOSFETs (LDMOS) are a promising technology for integrated mixed signal and mixed voltage applications for space.<sup>1-5</sup> Before these devices can be flown on long term space exploration missions, their radiation response must be understood. Although radiation is expected to produce only a modest shift in the threshold voltage of the thin gate oxides, the thicker buried oxides (BOX) may still be susceptible to radiation degradation. It has been recently shown that the operation and performance of LDMOS devices are strongly influenced by the back gate (substrate) voltage. For these devices, the back gate voltage modifies not only the parasitic back channel, but the series resistance of the drift region as well.<sup>3,4</sup> In this abstract, we show that the radiation induced degradation of LDMOS device operation involves several mechanisms and is more complex than the usual case of low-voltage SOI CMOS transistors.

Shown in Fig. 1 is a cross section of an nLDMOS device fabricated with a partially depleted 0.35 $\mu$ m commercial SOI technology. Approximate thickness ranges for the gate oxide, silicon film, and BOX are  $t_{\text{gox}} = 7-10\text{nm}$ ,  $t_{\text{Si}} = 100-300\text{nm}$ , and  $t_{\text{BOX}} = 200-500\text{nm}$ . The channel and drift regions are both 4 $\mu$ m long and the body is tied to source. Devices were irradiated with <sup>60</sup>Co  $\gamma$  rays in sequential steps from 10krad to 200krads at 2.5-5.0 rads/sec with  $V_s = V_d = 0\text{V}$ ,  $V_{g1} = 4\text{V}$ , and  $V_{g2} = 50\text{V}$ , corresponding to worst case bias conditions.

In Fig. 2,  $V_{\text{th1}}$  (front threshold) and  $V_{\text{th2}}$  (back-channel threshold) are plotted vs. dose. As expected, there is negligible degradation of the gate oxide. On the other hand, the large negative shift of  $V_{\text{th2}}$  ( $V_{\text{th2}}$  is less than 0V after 25 krad) indicates extensive positive charge trapping in the BOX.

In Fig. 3, pre- (solid) and post- 50krad (dashed) traces of  $I_d$  vs.  $V_{g1}$  for various  $V_{g2}$  (back gate) are shown. Before irradiation,  $I_d(V_{g1})$  characteristics are strongly influenced by  $V_{g2}$ . It has been previously found that  $V_{G2}$  modulates the series resistance ( $R_s$ ) and activates the parasitic back channel.<sup>3,4</sup> Three different regions of operation are distinguished.<sup>3,4</sup>

**Region 1 ( $V_{g2} < -40\text{V}$ ):** The back-channel is accumulated and the bottom of the drift region is inverted. The depletion width in the drift region is maximum.  $R_s$  is constant.  $I_D$  vs.  $V_{G1}$  remain identical.

**Region 2 ( $-40 < V_{g2} < +50 \text{V}$ ):** The back channel is still off but the depleted part of the drift region shrinks with  $V_{g2}$ . As  $R_s$  decreases,  $I_d$  and  $g_{\text{ml}}$  in strong inversion

both increase with  $V_{g2}$ .

**Region 3 ( $V_{g2} > +50 \text{V}$ ):** The Si/BOX interface is strongly inverted in the channel and strongly accumulated in the drift region. The contribution of the back channel to  $I_d$  is constant when the front channel is off and gradually decreases in strong inversion.  $g_{\text{m}}$  decreases with  $V_{g2}$  due to back channel conduction.

After irradiation, the modulation of  $I_d$  by  $V_{g2}$  is still present, but significantly reduced due to a narrower range of  $R_s$ . Using the model developed in [3,4] to extract  $R_s$ , it is seen in Fig. 4 that  $R_s$  decreases with dose at negative  $V_{g2}$ . At high doses, a negative  $V_{g2}$  is no longer enough to deplete the drift region, which remains accumulated due to the large amount of positive charge in the BOX. The transconductance, plotted vs. dose in Fig. 5, increases with total dose for  $-60\text{V} < V_{g2} < -40\text{V}$ . This increase is not due to an increase of mobility but rather to the reduction of  $R_s$  as positive charge builds up in the BOX. For  $V_{g2} > -40\text{V}$ ,  $g_{\text{m(max)}}$  decreases with dose.

The subthreshold swing,  $S1$ , of the front channel, increases slightly with dose (Fig. 6). Pre and post 50 krad traces of  $I_d$  vs.  $V_{g2}$  for various  $V_{g1}$  are shown in Fig. 7. These back-gate curves will be explained by changes in trap density, mobility and series resistance.

Finally, in Fig. 8, it is seen that the pre-rad junction breakdown voltage,  $V_{\text{bd}}$ , is also a function of  $V_{g2}$ . For  $V_{g2} < 0\text{V}$ ,  $V_{\text{bd}}$  peaks around  $V_{g2} = -30\text{V}$  as the bottom of the drift region becomes depleted and then begins to drop off below  $-30 \text{V}$  (i.e., bottom of the drift region inverted and back-channel accumulated). For  $V_{g2} \geq 0\text{V}$ ,  $V_{\text{bd}}$  decreases with  $V_{g2}$  as the bottom of the drift region accumulates and  $R_s$  decreases. The fact that  $R_s$  decreases with dose (Fig. 4) indicates that radiation may reduce the breakdown voltage of these devices.

In conclusion, the modulation of the series resistance of the drift region by the charge trapped in the BOX is the key effect which explains the radiation-induced degradation of LDMOSFETs as well as the difference between high-voltage and low-voltage SOI devices. Our models allow prediction of the front and back channel degradation during irradiation.

The authors wish to thank A. Johnston for valuable technical discussions. The work described here was carried out under contract with the National Aeronautics and Space Administration (NASA).

1. J.M. O'Connor, V.K. Luciani, and A.L. Caviglia, 1990 IEEE Int. SOI Conf. Proc., p. 167 (1990).
2. S. Cristoloveanu and S.S. Li, Electrical

Characterization of SOI Materials and Devices, Kluwer, (1995).

3. J.G. Fiorenza, J.A. del Alamo, and D.A. Antoniadis, 1999 IEEE Int. SOI Conf. Proc. p. 96 (1999).
4. A. Vandooren, S. Cristoloveanu, M. Mojarradi and E. Kolawa, IEEE Trans. on Electron. Dev. (2001).

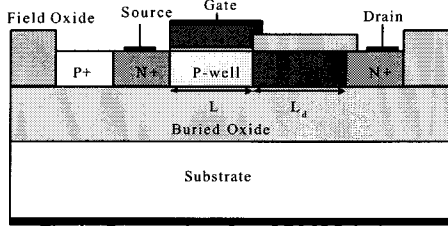


Fig. 1: Cross section of an nLDMOS device.

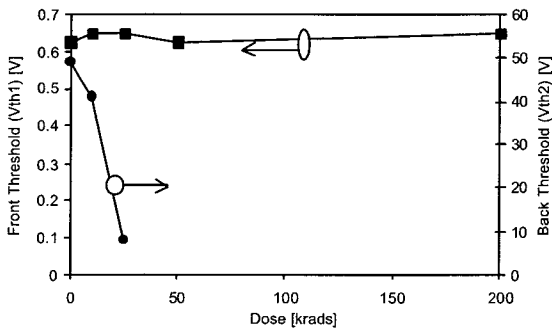


Fig. 2: Front threshold (V<sub>th1</sub>) and back threshold (V<sub>th2</sub>) vs. dose.

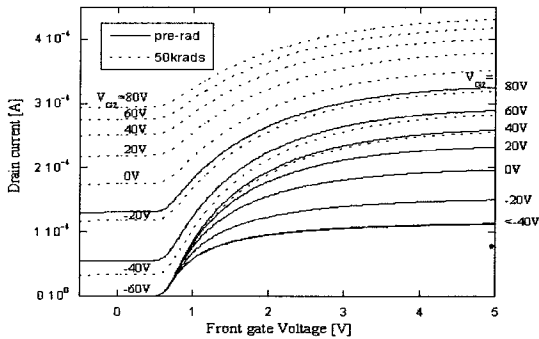


Fig. 3: Pre (solid) and post 50 krad (dashed) traces of I<sub>d</sub> vs. V<sub>g1</sub> for various V<sub>g2</sub>.

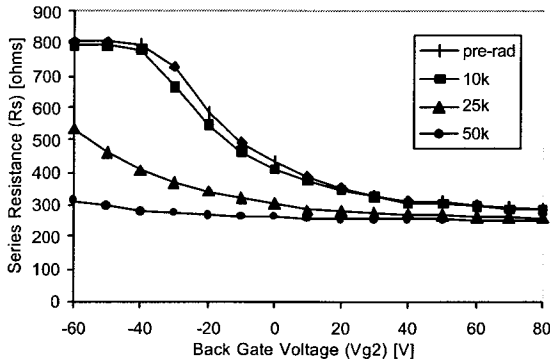


Fig. 4: R<sub>s</sub> vs. V<sub>g2</sub> for various radiation doses.

5. A. Vandooren, S. Cristoloveanu, M. Mojarradi and E. Kolawa, in Proc. of 199<sup>th</sup> Electrochemical Society Meeting (Washington, 2001).

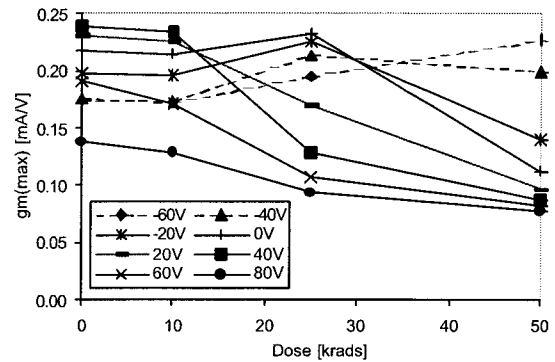


Fig. 5: g<sub>m</sub>(max) vs. dose for various V<sub>g2</sub>.

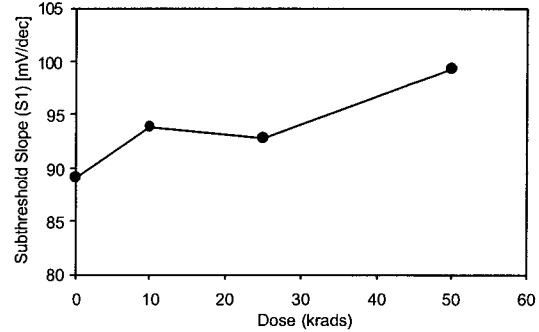


Fig. 6: Subthreshold slope, S, vs. dose.

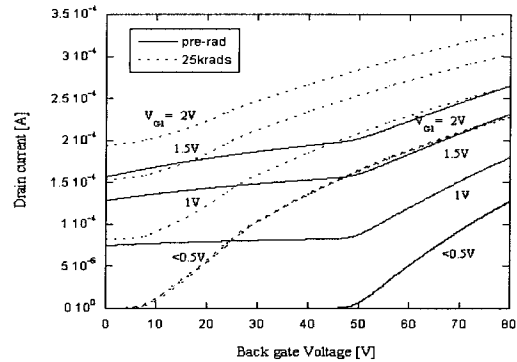


Fig. 7: Pre and post 50 krad traces of I<sub>d</sub> vs. V<sub>g2</sub> for various V<sub>g1</sub>.

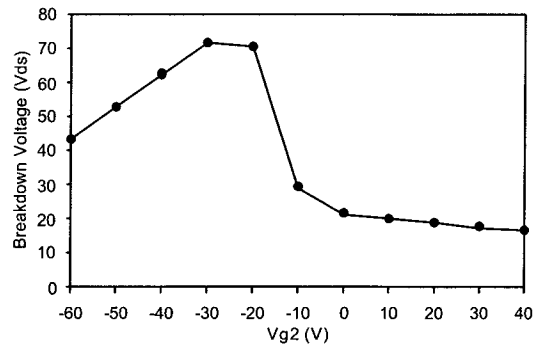


Fig. 8: Breakdown voltage vs. V<sub>g2</sub>.